

Design of An Inspection Robot System with Hybrid Operation Modes for Power Transmission Lines

Han Wang^{1,3}, En Li¹, Guodong Yang¹, Rui Guo²

1. The State Key Laboratory of Management and Control for Complex Systems ,
Institute of Automation, Chinese Academy of Science, Beijing 100190, China
 2. State Grid Shandong Electric Power Company, Jinan 250001, China
 3. University of Chinese Academy of Sciences, Beijing 100049, China
- {wanghan2018, en.li, guodong.yang}@ia.ac.cn, guoruihit@qq.com

Abstract – In this paper, we design a kind of transmission line inspection hybrid robot with a novel mechanical structure, taking the advantages of climbing robots and unmanned aerial vehicle(UAV). The hybrid robot has amphibious functions of on-wire crawling and flight. When encountering obstacles, the hybrid robot takes off directly to fly over them and it runs on the ground wire by rolling on wheels in the absence of obstacles. And then we verify its on-wire-balance by mechanical analysis. In order to achieve a tradeoff between the selection of the lightweight material and operational reliability of the robot, the finite element static structure simulation and dynamic simulation are carried out for important parts of the robot. In addition, a ROS-based robot control system has been designed and a multi-mode switching control strategy has been proposed.

Index Terms - Power line inspection robot; Mechanism design; Mechanical analysis; Simulation analysis; Multi-mode switching.

I. INTRODUCTION

At present, overhead transmission lines are the main way of power transmission. In order to ensure the safety of power supply, it is necessary to carry out regular inspection and maintenance of power lines to identify problems that endanger the safety of transmission [1]. Nowadays, the regular inspection of transmission lines is still mainly done by manpower, which has problems such as high labor intensity, low inspection efficiency, and high safety risks [2,3]. With the development of robot technology, advanced robots, drones, and other equipment have begun to be used in the field of power line inspection.

In recent years, the climbing robot which is suspended on the power line has been a hot research topic in the field of power line inspection robots. Climbing robots can move on the line by rolling or climbing and use the detection equipment to detect power line faults. Pouliot et al. from Hydro-Quebec, Canada, designed the Linescout robot for high-voltage power lines detection, which successfully overcame obstacles such as suspension clamps and vibration dampers on the line [4]. However, due to the weight up to 98 kg and complex mechanical structure, it took a long time and low efficiency to overcome obstacles. The Expliner robot [5] developed by Debenest et al., which owned highly-efficient

obstacle negotiation, was applied in the inspection of four-cracking type conductors. When it came to suspension clamps, the robot adjusted the position of gravitative center so that the two parts of the body passed through the obstacles. But it was a pity that the robot cannot work across the tower. There are also representative achievements in China, research institutions such as the Chinese Academy of Sciences and Wuhan University have also carried out a series of studies on climbing robots [6-8]. These robots were able to run stably online and performed tasks, and can overcome some obstacles. However, limited by mechanical structures, there was still some problems like low efficiency in obstacle negotiation and inability to work across the tower.

With the increasing popularity of unmanned aerial vehicle technology, the UAV has gradually been applied in the field of power line inspection in recent years [9-12]. For the convenience of description, we call it flying robot. Flying robot conducted transmission line fault detection by hovering near or along the line, and the new mechanical structure made it perform very well in obstacle negotiation. Compared with the climbing robot, the major superiority of flying robot lies in the wider movement space and strong flexibility. Besides being able to work across towers, the robot can get on and off the line easily without any auxiliary equipment. However, the flight time of the robot is limited by the battery capacity during the inspection mission in the air. Hence, flying robots can only work in small regions.

Combined with the advantages of flying robots and climbing robots, we designed a kind of transmission line inspection robot with a novel mechanical structure, which is called hybrid robots [13]. When encountering obstacles, the hybrid robot takes off directly and overcomes them. Without obstacles, it runs on ground wire by rolling on wheels. In addition, when it is on the wire, the motor providing lift is directly turned off to reduce power consumption so as to achieve longtime inspection. Hence, hybrid robots have the advantages of climbing robots when rolling on power lines, such as being able to close-distance detection on wires; It can also take off and land vertically like a drone, fly directly over obstacles, and conduct a detailed inspection of towers by hovering around them.

In this paper, we designed a novel hybrid robot system based on the DJI M600 UAV which was the flight platform. The rest of the paper is organized as follows: Section II presents the mechanical structure design of hybrid robot and verifies the balance of the robot on ground wire. Section III analyzes and calculates the static and dynamic forces of the robot on ground wire. Section IV carries on the static structure simulation and dynamics simulation of key components. Section V describes the control system design of hybrid robot and the control strategy of multi-mode switching. Finally, conclusions are depicted in Section VI.

II. MECHANICAL STRUCTURE OF HYBRID ROBOT

A. Design of the Mechanical Structure

Hybrid robots are mainly composed of the UAV and a patrol-line mechanism. Fig.1 shows the mechanical structure of the hybrid robot. The patrol-line mechanism is located in the below of UAV, which is used to land on ground wire and on-wire crawling. And the mechanism is divided into a clamping motion unit and a crawling drive unit, which meet the movement requirements of being able to clamp and release the wire as well as crawling back and forth. In addition, the battery pack is installed at the bottom of the drone landing gear to lower the robot's center of gravity. The patrol-line mechanism is connected to the drone through the upper four flange connectors, and the components of the hybrid robot are symmetrically arranged to ensure that the center of gravity is at the center line of the robot.

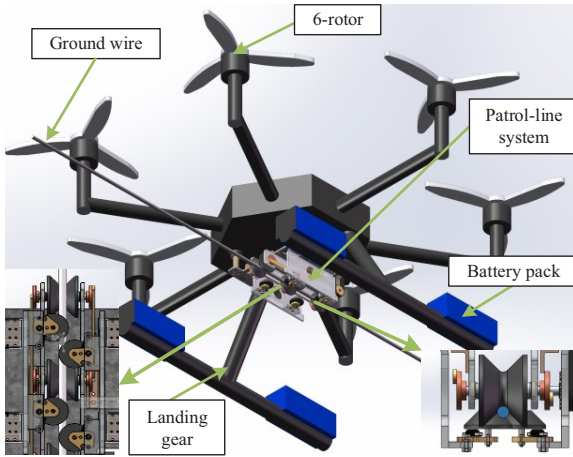


Fig.1. The mechanical structure of hybrid robot

The clamping movement of the patrol-line mechanism is realized by the rotation of the bi-directional sliding lead screw and the movement of the clamping wheel mechanism along the rolling guide rail, as shown in Fig.2. A pair of LM rolling guide rail is installed at the front and back of the mechanism, and the bottom of the guide rail is connected to the connecting plate. Besides, the screw nut is connected to the slide block of the guide rail. Hence, the rotation of the bi-directional sliding lead screw can make the slide blocks on both sides of the guide rail move towards each other in

opposite directions, and then realize the movement of clamping the wire with clamping mechanism. However, the motor used for clamping motion is so heavy that it affects the balance of robot's gravity. In order to ensure that the center of gravity of the mechanism is located in the center line, the motor and the bi-directional sliding lead screw are connected by bevel gear transmission to satisfy the gravity balance.

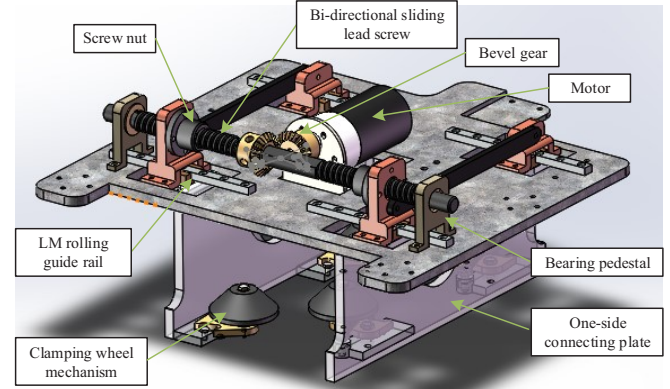


Fig.2. The mechanical structure of clamping action

The design of the clamping wheel mechanism mainly considers two aspects: 1) as clamping the wire, the supporting force to the ground wire should also be provided, so that the normal pressure between the driving wheel and the ground wire can be increased to increase the friction force and avoid slipping caused by insufficient friction force; 2) elastic elements should be designed in the clamping wheel mechanism to improve the adaptability of the mechanism to ground wires with different diameters and the function of absorbing impact load. Based on the above-mentioned factors, designed the clamping wheel with a 45-degree bevel shape, so that the normal pressure between the wire and the driving wheel can be increased when the ground wire is clamped. In addition, the extension spring with pretension force is considered in the clamping wheel mechanism. As the movement is gentle, the clamping wheel is pulled to the fixing place of the limit bolt by the extension spring. When the movement state changes, the clamping wheel can rotate around the rotating bolt to absorb the impact. Finally, when the movement returns to a stable state, the clamping wheel is restored to its original position by the pretension force.

The crawling drive unit uses a three-crank mechanism to realize the linkage between the drive wheels to enhance the driving effect, as shown in Fig.3. In addition, the synchronous belt is selected to transmit the torque of the motor. The upper end of the synchronous belt is connected to the driving motor, while the lower end is connected to the extended driving shaft. After the motor torque is transmitted to the driving wheel, each wheel becomes the driving wheel through a three-crank mechanism. At the same time, the structure ensures that the driving motor can be installed in the center line of the mechanism, avoiding the asymmetric weight distribution of the robot.

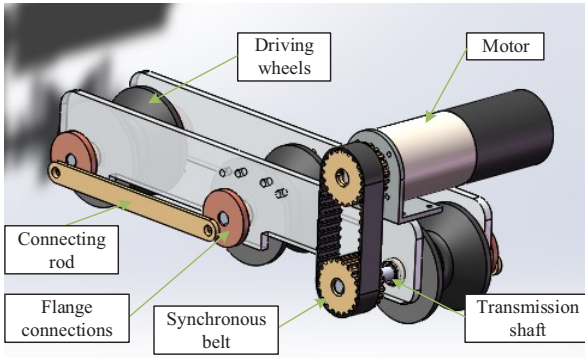


Fig.3. The mechanical structure of climbing

B. On-wire Balance Analysis

It must be satisfied that the overall center of gravity of the robot is below the wire and its center of gravity should be as low as possible, to ensure that the hybrid robot can be balanced on the wire. Therefore, the DJI M600 battery pack is modified from the upper part of the drone to the bottom of the landing gear, and the weight of the upper part of the drone is reduced as much as possible. After the actual weighing in the laboratory, the total weight of the DJI M600 (including the battery pack) is about 9.6kg, while the weight of the battery pack exceeds 1/2 of the weight of the drone (excluding the battery pack). Hence, the modification of the battery below the wire can effectively reduce the height of the center of gravity.

Fig. 4 is the force diagram of the hybrid robot located on the ground wire. Suppose that the robot is deflected by an angle θ from the vertical direction, and point B is the point of contact between the robot and the wire. Point A is the center of gravity of the robot above the earth wire, while point C and point D are the centers of gravity of the battery pack below the ground wire respectively. The values of each parameter are shown in Table I.

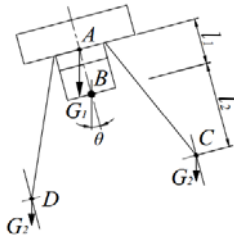


Fig.4. Force analysis of the robot on the line

According to the torque balance equation, in order to avoid the instability of the robot, the following conditions must be satisfied,

$$m_1 g \sin \theta \times l_1 < m_2 g \sin \theta \times l_2 \quad (1)$$

m_1 and m_2 are respectively the weight of the robot above and below the wire, of which the upper total weight includes the UAV (excluding the battery pack) with about 6kg and the patrol-line mechanism with about 3kg. Then the calculated weight of the robot below the line should meet $m_2 > 4.86\text{kg}$. Hence, a battery pack weighing no less than 4.86kg only

needs to be installed at the bottom of the landing gear to meet the balance requirement of the robot on the wire.

III. MECHANICAL ANALYSIS OF THE ROBOT

The hybrid robot moves on the ground wire. In this paper, the maximum crawling angle of the robot is 15° , and the static and dynamic mechanical analysis is carried out.

A. Static Mechanical Analysis

After the robot lands on the wire, the clamping unit provides the clamping force between the patrol-line mechanism and the ground wire, so that the robot can rest on the wire.

Fig. 5 is a force analysis of the robot resting on the wire at 15° . In Fig. 5, the robot is subject to its own gravity G , the normal pressure N_m exerted on the three driving wheels, the friction f_l exerted on the three driving wheels along the ground wire, and the reaction force of the pressure on the clamping wheel is N_z' in the vertical direction. The clamping wheel is free from friction while the robot is resting on the wire.

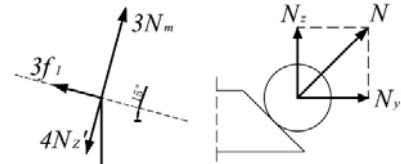


Fig.5. Static force analysis

Supposed that the friction coefficient between the ground wire and the driving wheel is μ , the following conditions should be satisfied when the robot is stationary on the wire,

$$3f_l \geq G \sin 15^\circ \quad (2)$$

$$f_l = \mu N_m \quad (3)$$

$$3N_m = 4N_z' + G \cos 15^\circ \quad (4)$$

$$N_z' = N \sin 45^\circ \quad (5)$$

Based on the above relations, the clamping force N required by the robot in the static state is obtained,

$$N \geq \frac{G}{2\sqrt{2}} \left(\frac{\sin 15^\circ}{\mu} - \cos 15^\circ \right) \quad (6)$$

B. Dynamic Mechanical Analysis

Figure 6 is a force analysis of the robot crawling upward along the wire at 15° .

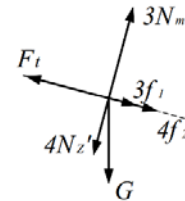


Fig.6. Force analysis of upward motion

Different from the static state, the robot is affected by the motor driving force F_t along the upward direction of motion,

as well as the friction force f_1 and f_2 in the driving wheel and clamping wheel along the opposite direction of motion, ignoring the influence of air resistance.

When the robot crawls on the line, the motor needs to provide sufficient driving force to overcome its own gravity and friction. But the driving force cannot be too great, otherwise will cause the driving wheel to slip. The limit value that the driving force can reach is called the adhesive force. The following is the formula for calculating the adhesive force.

$$F_t \leq F_\phi = \varphi \cdot 3N_m \quad (7)$$

Where, φ is the adhesion coefficient, which is determined by the surface material of the driving wheel and the ground wire. Then, in the process of robot movement, the following conditions must be met,

$$F_t \geq 4f_2 + 3f_1 + G \sin 15^\circ \quad (8)$$

$$3N_m = 4N_z + G \cos 15^\circ \quad (9)$$

$$f_1 = \mu N_m$$

$$f_2 = \mu N$$

Based on the above conditions, the driving force when the robot crawls upward along the wire at 15 degrees should satisfy the following conditions,

$$F_t \leq \varphi(2\sqrt{2}N + G \cos 15^\circ) \quad (10)$$

$$F_t \geq 4\sqrt{2}\mu N + (\mu \cos 15^\circ + \sin 15^\circ)G$$

Table I shows the corresponding values of the parameters in the above robot mechanical analysis, as well as the calculated minimum clamping force N and minimum motor driving force F_t .

TABLE I
PARAMETER VALUES IN MECHANICAL ANALYSIS

Symbol/unit	value	Symbol/unit	value
G/kg	15	N/N	40.28
m_1/kg	9	N_m/N	86.27
m_2/kg	6	f_1/N	12.94
l_1/cm	15	f_2/N	6.40
l_2/cm	28	φ	0.85
μ	0.15	F_t/N	94.73

According to the clamping force N and motor driving force F_t obtained above, and in accordance with the motor speed and other requirements, the torque and power of the motor required for the clamping motion and the crawling motion can be calculated. Finally, the motor is selected according to the requirements such as structure size.

IV. SIMULATION ANALYSIS OF KEY PARTS

Hybrid robots use the drone as the flight platform, so it is necessary to select the material on lightweight to strictly limit the overall weight of the robot. However, in the process of

operation, if the component structure changes due to material strength problems, it is bound to affect the stability and reliability of the robot. Hence, the static structure and dynamic simulation of key parts in the mechanism are carried out in this section.

A. Static Structure Simulation

As an important part to transmit power, the transmission shaft affects the normal operation of the mechanism. In this paper, a transmission shaft connected to the synchronous belt pulley and also the longest one is selected for static structure simulation. The position and force of the transmission shaft are shown in Fig. 7.

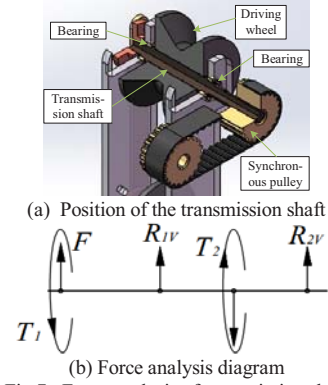


Fig. 7. Force analysis of transmission shaft

In Fig. 7 (b), N is the normal pressure on the drive shaft, R_{1V} and R_{2V} are the supporting force of the bearing on the drive shaft, T_1 and T_2 are the input torque and output torque of the drive shaft, and F is the tension force of the synchronous belt pulley. In this paper, 40Cr is selected as the material of the transmission shaft for static structure simulation. After finite element analysis, the equivalent stress diagram and total deformation diagram of the transmission shaft are obtained, as shown in Fig. 8.

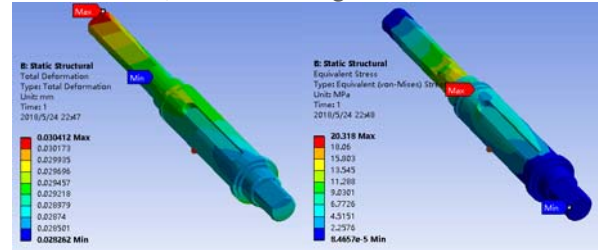


Fig. 8. The deformation and equivalent stress of transmission shaft

It can be found from the equivalent stress diagram that the maximum stress occurs at the shoulder of the elongated end of the long shaft, and the maximum stress is 20.318MPa, less than one-tenth of the allowable stress of the material. In addition, the maximum deformation in the total deformation diagram is 0.030412mm, while the minimum radius of the shaft is 8mm, so the relative deformation is very small. And the deformation in that position has no great influence on the normal transmission. Hence, the deformation is also within the safe range.

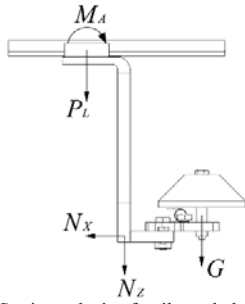


Fig.9. Static analysis of unilateral clamping unit

The connecting plates on both sides of the patrol-line mechanism are not only the main frame of the mechanism, but also the important connecting parts of the upper rolling guide rail and the lower clamping wheel mechanism. The forces in Fig. 9 include: G is the gravity of the clamping wheel mechanism, N_x and N_y are the horizontal and vertical components of the reverse pressure on the clamping wheel, M_A and P_L are the pitching moment and the reverse radial load generated by the slider respectively.

Through the static analysis of the one-side clamping unit above, Fig. 10 shows the equivalent stress diagram and total deformation diagram obtained after the static structure simulation of the one-side clamping plate. It can be seen from the stress diagram that the maximum stress is 34.86MPa , which is less than the yield limit. Moreover, the maximum deformation obtained from the deformation diagram is 1.95mm , so the influence of this deformation on the clamping movement can be ignored. Therefore, the selection of lightweight carbon fiber materials can meet the requirements of use.

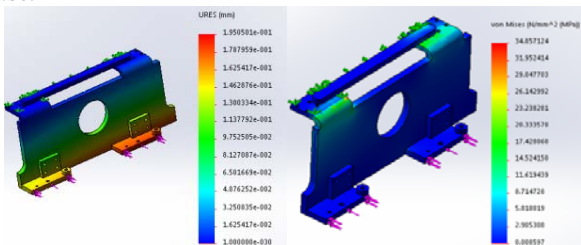


Fig.10. The deformation and equivalent stress of one-side connecting plate

B. Dynamic Structure Simulation

By increasing the clamping force, the robot can provide sufficient friction force to guarantee that the robot can crawl on the wire at a given angle. Besides, elastic parts are designed in the clamping wheel mechanism to improve the reliability of the robot. The spring stiffness is taken as the main parameter of the elastic component. If the spring stiffness is not enough, the clamping wheel with a small impact load on the mechanism will cause greater displacement, affecting the normal operation of the mechanism. If the spring stiffness is too large, then the impact load on the mechanism cannot be absorbed, and the robot cannot adapt to the ground wire with different diameters, at the same time, the performance of obstacle negotiation will also be affected. So it is very important to

choose the right parameters of the spring for the mechanism. Hence, this paper uses SolidWorks Motion to analyze the clamping wheel mechanism by dynamic simulation. Set the structural size parameters of the spring as the outer diameter of 5.00mm , the winding number of 25, wire diameter of 0.50mm , take the free length of the spring as 20mm and then simulate the effect of external load, finally determine the tension spring parameters meet the conditions by changing the spring parameters.

According to the maximum clamping force of the clamping wheel in the horizontal direction calculated by the static mechanics analysis in the third section above, as well as the contact and fit conditions of various parts of the clamping mechanism and other constraints, a set of displacement-time curves of the clamping wheel with different spring stiffness were obtained through dynamic simulation, as shown in Fig. 11. It can be seen from Fig. 11 that the clamping wheel has different displacements for springs with different stiffness. Tension springs with a stiffness range of $10\sim 12\text{N/mm}$ are selected for better movement effect.

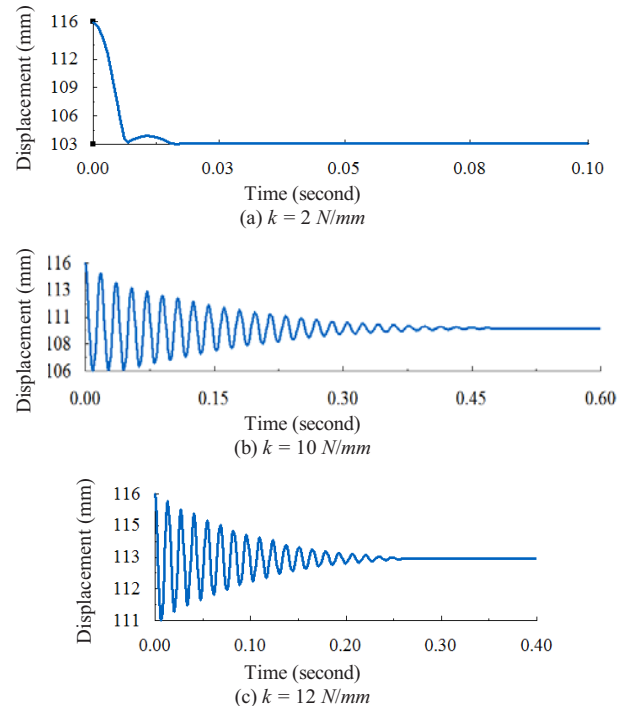


Fig.11. Displacement - time curve of clamping wheel with different spring stiffness

V. CONTROL SYSTEM

Fig. 12 shows the control system structure diagram of the robot. The main controller is NVIDIA Jetson TX2, in which ROS is run to realize the information interaction between devices in the control system. The data and information collected by the camera and radar are processed by TX2, and the patrol-line system and UAV platform are controlled to realize the multi-mode switching strategy of the robot.

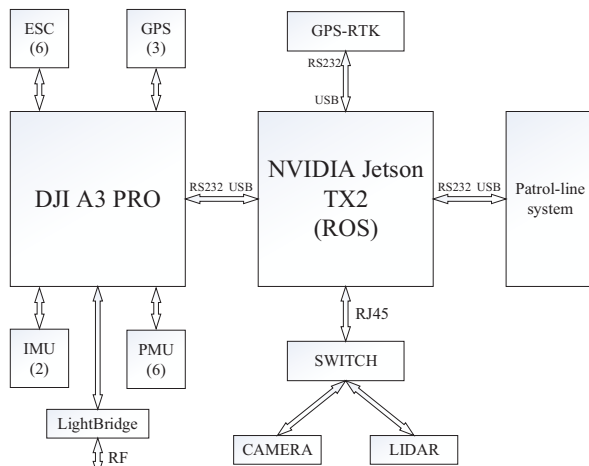


Fig.12. Structure diagram of robot control system

The multi-mode switching strategy is shown in Fig. 13. When the ground wire is not detected by the system, the control is assigned to the flight control platform. According to real-time positioning and radar detection of the location of the wire, flight control is performed to bring the robot close to the wire and accurately land on it, after which, the control power is transferred to the patrol-line system controlling the robot to crawl along the wire. When an obstacle is detected by the robot through real-time detection by radar and camera in the process of running on the wire, the control power is transferred again controlling the robot flies over the obstacle. After the obstacle is overcome, the robot is controlled again to land and crawl on the wire until the end of the mission.

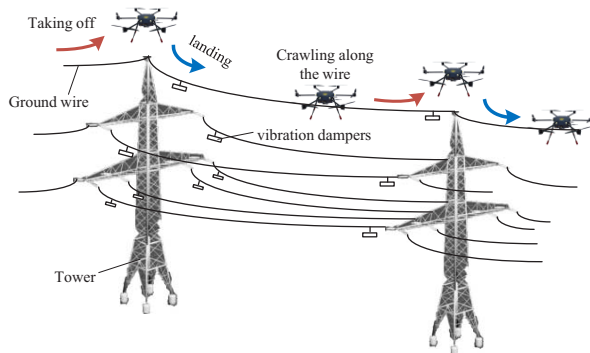


Fig.13. Movement schematic diagram of multi-mode control strategy

VI. CONCLUSION

In allusion to existing deficiency of climbing robots and flying robots in the field of power line inspection, a novel hybrid robot system is designed in this paper. Based on DJI M600 UAV, the hybrid robot is divided into flight system and patrol-line system. It has symmetrical structure and functions of amphibious movement such as crawling on the wire and flying. As moving on the wire, it can also satisfy the on-wire balance requirement of the robot. Through mechanical analysis and static structure simulation of key parts, this paper verifies that the transmission shaft and one-side

clamping unit can meet the strength requirements while ensuring the lightweight material selection. Meanwhile, the parameters of the spring for the normal operation of the clamping wheel mechanism are obtained by dynamic simulation.

In addition, based on the mechanical structure of the hybrid robot, its control system has been designed. A multi-mode switching control strategy is proposed to realize the efficient and flexible power line inspection with the hybrid robot. In the future, it is necessary to optimize its mechanical structure and improve the control strategy and method of the robot in operation based on the actual experiment of the prototype.

ACKNOWLEDGMENT

This work is supported by the National Key R&D Program of China (No. 2018YFB1307400) and National Natural Science Foundation of China (No. U1713224).

REFERENCES

- [1] F. Zhou, A. Wu, Y. Li, J. Wang and Z. Liang, "Development of a mobile robot for high voltage overhead power transmission lines," *Automation of Electric Power Systems*, vol.23, pp. 89-91, 2004.
- [2] J. Katrasnik, F. Pernus and B. Likar, "A Survey of Mobile Robots for Distribution Power Line Inspection," *IEEE Transactions on Power Delivery*, vol.25, no.1, pp.485-493, 2009.
- [3] A. Pagnano, M. Hopf and R. Teti, "A roadmap for automated power line inspection maintenance and repair," *Procedia Cirp*, vol. 12, pp.234-239, 2013.
- [4] N. Debenest, P.L. Richard and S. Montambault, "LineScout Technology Opens the Way to Robotic Inspection and Maintenance of High-Voltage Power Lines," *IEEE Power & Energy Technology Systems Journal*, vol.2, no.1, pp.1-11, 2015.
- [5] P. Debenest, M. Guarnieri, K. Takita, E.F. Fukushima, S. Hirose, K. Tamura, A. Kimura, H. Kubokawa, N. Iwama, and F. Shiga, "Expliner - Robot for inspection of transmission lines," in *Proc. IEEE International Conference on Robotics and Automation*, 2008, pp. 3978-3984.
- [6] G. Wu, X. Xiao, H. Xiao, J. Dai and Z. Huang, "Motion Planning of Non-collision Obstacles Overcoming for High-Voltage Power Transmission-Line Inspection Robot," in *Proc International Conference on Intelligent Robotics and Applications*, 2008, pp. 1195-1205.
- [7] X. Yue, H. Wang, Y. Jiang, N. Xi and J. Xu, "Research on a novel inspection robot mechanism for power transmission lines," *IEEE International Conference on Robotics and Biomimetics (ROBIO)*, 2015, pp. 2211-2216.
- [8] L. Tang, S. Fu, L. Fang and H. Wang, "Obstacle-navigation strategy of a wire-suspend robot for power transmission lines," *IEEE International Conference on Robotics and Biomimetics*, 2004, pp. 82-87.
- [9] X. Peng, Z. Liu, X. Mai, Z. Luo, K. Wang and X. Xie, "A transmission line inspection system based on remote sensing: system and its key technologies," *Remote Sensing Information*, vol.41, no.10, pp.117-122, 2017.
- [10] S. Huang, X. Gu, J. Zhang, "Design of new oil moving fixed-wing unmanned aerial vehicle for power line patrolling," *Automation of Electric Power Systems*, vol.38, no.04, pp.104-108, 2014.
- [11] L. Matikainen, M. Lehtomäki, E. Ahokas, J. Hyypä, M. Karjalainen, A. Jaakkola, A. Kukko, and T. Heinonen, "Remote sensing methods for power line corridor surveys," *ISPRS Journal of Photogrammetry and Remote Sensing*, vol.119, pp.10-31, 2016.
- [12] M. Shi, K. Qin, K. Li, and Y. Zheng, "Design and testing on autonomous multi-UAV cooperation for high-voltage transmission line inspection," *Automation of Electric Power Systems*, vol.41, no.10, 2017.
- [13] W. Chang, G. Yang, J. Yu, Z. Liang, L. Cheng and C. Zhou, "Development of a power line inspection robot with hybrid operation modes," *IEEE/RSJ International Conference on Intelligent Robots and Systems (IROS)*, 2017, pp. 973-978.